Contribution from the Department of Chemistry and Division of Engineering, Brown University, Providence, Rhode Island 02912

Preparation, Crystal Structure, and Properties of $NH_4V_3O_6F$

F. PINTCHOVSKI, S. SOLED, and A WOLD*

Received July 24, 1975 AIC50535V

Single crystals of $NH_4V_3O_6F$ have been synthesized by allowing ammonium vanadate, vanadium metal, and ammonium hydrogen fluoride to react under a hydrostatic pressure of 1.33 kbars at 450°C. The product crystallizes in the monoclinic system, space group $P2/c$, with a_0 = 8.251 (4) Å, b_0 = 4.939 (1) Å, c_0 = 6.986 (1) Å, and β = 100.5 (3)°; ρ_{calcd} = 3.39 g cm^{-3}, ρ_{exptl} = 3.36 (2) g cm^{-3} for Z = 2. The structure consists of octahedra linked together by corner, edge, and face sharing to form 6 Å thick sheets that extend parallel to (100). Between these sheets there are zigzag chains of ammonium ions. The compound exhibits Curie–Weiss behavior between 240 and 450 K, with a P_{eff} of 1.83 BM, and has a room-temperature resistivity of 10^8 Ω-cm, indicating the localized character of the electrons.

Introduction

The large number of vanadium oxides, oxyfluorides, and vanadates exist in a variety of structural types and vanadium oxidation states and exhibit a wide range of physical properties. The vanadium atoms can be coordinated in a tetrahedral,[1,2] a square-pyramidal,[3] a trigonal-bipyramidal,[4,5] or an octahedral manner,[6] and the coordination polyhedra can share either edges, corners, or faces. The oxidation states of vanadium can vary from +5 (d^0, as found in V_2O_5[4]) to +2 (d^3, as found in VO[7]). Distances between vanadium atoms in linked polyhedra range from 2.62 to 3.29 Å,[8] and Goodenough has suggested that this is an important factor in accounting for the wide spectrum of physical properties exhibited by different vanadium oxides.[9] In octahedra that share common edges or faces, there is the possibility of electron delocalization resulting from the overlap of metal t_{2g} orbitals, if the metal–metal approach is less than a critical value; for the oxides with V^{3+} and V^{4+} the critical vanadium–vanadium separation is ~2.9 Å. In octahedra that share corners, cation–anion–cation interactions can also delocalize the 3d electrons if the covalent mixing of the oxygen 2s and 2p orbitals with the vanadium e_g orbitals is large. In addition, a ferroelectric-type distortion can occur if the vanadium atoms are displaced from their octahedral sites.

Since fluorine and oxygen have similar ionic radii (r_{F^-} = 1.33 Å, $r_{O^{2-}}$ = 1.40 Å[10]), it has been possible to substitute fluorine for oxygen in some transition metal oxides. In the vanadium–oxygen–fluorine system, several different synthetic methods have been used. For example, Reynolds[11] and Chamberland,[12] working independently, successfully substituted up to 0.21 mole % fluorine into vanadium(IV) oxide by allowing under hydrothermal conditions vanadium(V) oxide, vanadium metal, and hydrofluoric acid to react at 600°C and 1.33 kbars. Galy[13] prepared the vanadium oxyfluoride bronzes $Na_xV_2O_{5-x}F_x$ by a direct solid-state reaction between vanadium(V) oxide, vanadium(IV) oxide, and sodium fluoride at 550°C, and Chamberland[14] utilized a tetrahedral anvil press to prepare VOF by allowing vanadium(III) oxide and vanadium(III) fluoride to react at 800–1100°C and 65 kbars.

A new synthetic technique based on the application of hydrostatic pressure to molten salts has been recently developed to prepare transition metal oxyfluorides. Crystals of $NH_4ReO_{1.5}F_3 \cdot H_2O$ have been synthesized by allowing ammonium perrhenate, rhenium metal, and ammonium hydrogen fluoride to react under hydrostatic pressure.[15] This synthetic technique has now been applied to the vanadium system, and crystals of a new vanadium oxyfluoride $NH_4V_3O_6F$ have been grown when ammonium vanadate, vanadium metal, and ammonium hydrogen fluoride reacted at 450°C and 1.33 kbars. The synthesis, characterization, structure, and physical properties of this new compound are described here.

Experimental Section

Preparation of Materials. $NH_4V_3O_6F$ single crystals were synthesized with a hydrothermal apparatus that has been described previously.[11] A mixture of ammonium vanadate (Fisher Scientific Co., twice recrystallized), vanadium metal (Gallard-Schlesinger), and ammonium hydrogen fluoride (Fisher Scientific Co., twice recrystallized) in the mole ratio 1:0.1:4 was placed in a thin-walled gold tube (5-mm i.d. × 10 cm) that was sealed previously at one end. The top of the tube was crimped shut and melt-sealed and the tube was placed in a steel pressure vessel. The temperature and pressure were monitored continuously and maintained within ±5°C and ±0.01 kbar, respectively. Black crystals were grown when the mixture was allowed to react at 450°C and 1.33 kbars for 7–10 days followed by cooling at a rate of 50°/hr.

Chemical Analysis. The fluoride ion concentration was measured with an electrode (fluoride ion activity electrode, Model 94-09, Orion Research, Inc.) specifically sensitive to this ion.[11]

The vanadium concentration was determined by the phenanthroline–ferrous ion method.[16] To determine the formal oxidation state of vanadium, the sample was dissolved in acid V^{5+} solution and the reduced vanadium was potentiometrically titrated with a standard $KMnO_4$ solution.[17] The ammonium ion was analyzed as ammonia, using a specific ion electrode (ammonia electrode, Model 95-10, Orion Research, Inc.).

Density Measurements. The density of the crystals was determined using a hydrostatic technique based on Archimede's principle[18] with the use of a Mettler H-54 analytical balance. Perfluoro(1-methyldecalin) (Pierce Chemical Co.) was the liquid medium and was first calibrated with a crystal of high-purity silicon (Gallard-Schlesinger, 99.999%), ρ = 2.328 (2) g cm^{-3}.

Magnetic Measurements. Magnetic susceptibility data over the range 4.2–450 K were obtained with a Faraday balance[19] at a field strength of 10.40 Oe. For the measurements between 300 and 450 K, the sample was encapsulated under vacuum[20] to avoid the possibility of oxidation. The susceptibility was also measured as a function of field strength (10.40–6.22 Oe) at 4.2 and 77 K to ascertain the presence of ferromagnetic impurities at low temperature. Susceptibility values were corrected for the core diamagnetism of V^{4+} (-7×10^{-6} emu/mol), NH_4^+ (-12.5×10^{-6} emu/mol), F^- (-11×10^{-6} emu/mol), and O^{2-} (-12×10^{-6} emu/mol).[21]

The effective paramagnetic moment and Weiss constant were determined from a least-squares refinement of the inverse susceptibility data over the temperature range 240–450 K.

Electrical Measurements. Electrical resistivity measurements were made on single crystals using the four-probe van der Pauw technique.[22] Indium leads were soldered ultrasonically to the crystals. The samples were mounted on blocks made from high-resistivity epoxy cement and the leads were then attached to gold terminals which were bound to the sample blocks.

Unit Cell and Intensity Data. Precession and Weissenberg photographs indicated that the compound crystallized in the monoclinic system, in either space group $P2/c$ or Pc. The lattice parameters were obtained at ambient room temperature from a least-squares refinement of the angular settings of 12 strong reflections centered on a Picker FACS-1 diffractometer that was equipped with a graphite monochromator and a Mo x-ray tube ($\lambda(K\alpha)$ 0.7107 Å). Table I lists the crystallographic data for the compound. To check the sample for the presence of any additional phases, ground crystals were examined by both fast (1° 2θ min^{-1}) and slow ($^1/_4$° 2θ min^{-1}) scan x-ray techniques using a Norelco diffractometer with monochromatic Cu $K\alpha_1$ radiation (λ 1.5405 Å).

The mosaicity of the crystal was examined by narrow-source, open-counter ω scans. The full widths at half-maximum for several

Table I

Crystallographic Data for $NH_4V_3O_6F$

System	Monoclinic		
a_0, Å	8.251 (4)	Z	2
b_0, Å	4.939 (1)	ρ_{calcd}, g cm^{-3}	3.39
c_0, Å	6.986 (1)	ρ_{exp}, g cm^{-3}	3.36 (2)
β, deg	100.5 (3)	μ(Mo Kα), cm^{-1}	51.9
Absences	$h0l$, l = $2n+1$	Crystal habit	Needle bounded by {001}, {110}, {100}
Space group	$P2/c$	Crystal size	0.21 mm × 0.10 mm × 0.06 mm

Symmetry Codes

No symbol	x	y	z
i	$\bar{x}$	$\bar{y}$	$\bar{z}$
ii	x	$-1+y$	z
iii	$\bar{x}$	$1-y$	$\bar{z}$
iv	$\bar{x}$	y	$1/2-z$
v	x	$1-y$	$\bar{z}$
vi	$\bar{x}$	$\bar{y}$	$1/2+z$
vii	$\bar{x}$	$-1+y$	$1/2-z$
viii	x	$\bar{y}$	$-1/2+z$
ix	x	$1-y$	$-1/2+z$
x	$\bar{x}$	$1+y$	z
xi	$\bar{x}$	$1+y$	$1/2-z$
xii	x	$1-y$	$1/2+z$
xiii	$1-x$	y	$1/2-z$
xiv	$1-x$	$1-y$	$1-z$

strong reflections were less than 0.1°. Single-crystal intensity data were collected on the FACS-1 over one quadrant of reciprocal space within the angular region $5° < 2\theta < 60°$. A symmetrical scan range in 2θ was used from −0.90 to +0.90° of the Mo Kα peak with allowances made for the Kα_1–Kα_2 separation. Attenuators were inserted automatically if the count rate of the diffracted beam exceeded approximately 9000 counts sec^{-1} during the scan. Structure amplitudes were calculated in the usual way. The variance in F_o^2 was estimated by the expression

$$v(|F_o|^2) = \sigma(|F_o|^2)^2 = (Lp)^{-2}[C + 0.83 + (t_c/2t_b)^2(B_1 + B_2 + 1.65) + (0.050)^2 + (0.05(B_1 + B_2))^2]$$

Where Lp is the Lorentz–polarization factor, C is the total integrated count obtained in time t_c, and B_1 and B_2 are the two background counts each obtained in time t_b. The intensities were corrected for absorption by means of the GONO 9 program;[23] transmission coefficients range from 0.64 to 0.78. Four hundred and sixty-nine reflections whose intensities were greater than twice their standard deviations were used in the subsequent least-squares refinements.

Solution and Refinement of the Structure. The structure was solved by standard heavy-atom methods and refined by least-squares methods with the program BULS, which is a local modification of the ORFLS[24] program. The function minimized was $w(|F_o| - |F_c|)^2$ with the weights taken as $w = 4F_o^2/w(F_o^2)$; this is just the reciprocal variance in $|F_o|$. In all calculations, the atomic scattering factors for the neutral atoms were taken from Cromer and Waber.[25] The effects of anomalous dispersion for the vanadium atoms were included in the calculated structure factors with the appropriate values of $\Delta f'$ and $\Delta f''$ taken from Cromer's report.[26]

The positions of the two independent vanadium atoms were located from a three-dimensional Patterson function. Initially, the centrosymmetric alternative $P2/c$ was chosen and the positional and isotropic thermal parameters of the V(1) and V(2) atoms were adjusted by least-squares refinement to give R = 33.2% and R_w = 41.1% based on observed F values. The oxygen and nitrogen atoms were found from a difference Fourier map. The fluorine atoms partially occupy one or more of the oxygen sites, so that the determination of the fluorine content was based solely on the chemical analysis. Consequently, in this and all future refinements, only the scattering factors for oxygen were included for oxygen and fluorine atoms. Further cycles of refinement with isotropic thermal parameters for all atoms yielded R = 12.3% and R_w = 13.3%. However, several disturbing features remained. A difference Fourier map revealed two regions of positive electron density near the V(1) atom at the inversion center (0, 0, 0). Although a refinement with anisotropic thermal parameters for the vanadium atoms lowered R to 5.6% (R_w = 6.8%, 32 variables), the thermal ellipsoid of V(1) was badly distorted with rms displacements ranging from 0.04 to 0.25 Å. The possibility that V(1) did not lie on an inversion center was tested by performing two refinements in the noncentrosymmetric space group Pc. In each case, the V(1) atom was displaced toward one of the regions of positive electron density (along the V(1)–O(1) bond) and the positional and anisotropic thermal parameters of the vanadium atoms along with the positional and isotropic thermal parameters of the other atoms were varied. R values of 5.2% (R_w = 6.2%, 58 variables) were obtained, but again, in both cases, the thermal ellipsoid of V(1) was extremely elongated in the same direction as before. It appeared that there was a disorder in the structure with V(1) partially occupying positions straddling the origin. An isotropic refinement in $P2/c$ with V(1) having a 50% occupancy in each of two positions, symmetrically disposed to and slightly displaced from the inversion center, was attempted. The residual dropped from the value of 12.3%, with V(1) on the inversion center, to 5.8% (R_w = 6.9%, 25 variables) and the isotropic temperature factor parameter of V(1) became nearly identical with that of V(2). Therefore, $P2/c$ was chosen as the correct space group. Because of the proximity of V(1) to the inversion center, anisotropic refinement of the thermal motion of V(1) in this model was not possible. A final difference Fourier map confirmed the structure and revealed that the hydrogen atoms of the ammonium ions were buried in the background noise. In Table II, the final positional and thermal parameters for the structure together with their standard deviations are listed. A tabulation of the final values of $|F_o|$ and $|F_c|$ (in electrons × 10) for the 469 reflections included in the refinement is available.[27]

Table II. Fractional Atomic Positional and Isotropic Thermal Parameters

Atom	x	y	z	B, Å^2
V(1)	0.0253 (3)	0.0095 (12)	0.0007 (5)	0.47 (5)
V(2)	−0.1617 (2)	0.4870 (4)	0.1228 (2)	0.47 (3)
O(1)	0.2061 (7)	0.1596 (11)	−0.0107 (8)	0.36 (9)
O(2)	0.1018 (7)	0.6636 (12)	0.1176 (8)	0.49 (9)
O(3)	0.0	0.1955 (17)	0.25	0.44 (13)
O(4)	0.3456 (8)	0.3692 (13)	0.3810 (9)	0.96 (11)
N	0.50	0.8899 (24)	0.25	1.10 (10)

Table III. Chemical Analysis

	Calcd	Found
% V	53.9	54.0 (1)
V oxidn no.	4.00	4.03 (2)
% N	5.97	5.95 (2)
% F	6.67	6.57 (4)

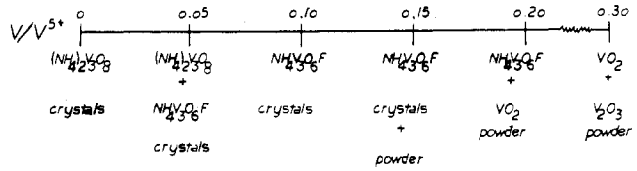

Figure 1. Effect of varying the V:V^{5+} molar ratio. Ammonium hydrogen fluoride was always present in excess.

Results and Discussion

Chemical Analysis. Table III compares the result of the chemical analysis with the calculated values based on the formula $NH_4V_3O_6F$.

Figure 1 shows the different phases obtained by varying the V:V^{5+} molar ratios under the conditions described in the Experimental Section. In all cases the ammonium hydrogen fluoride was present in excess. The best growth conditions for $NH_4V_3O_6F$ occurred when the V:V^{5+} molar ratio was 0.10.

Description of the Structure. The crystal structure of $NH_4V_3O_6F$ can be visualized in terms of either the cation or the anion coordination polyhedra; the former will be considered first. The two crystallographically independent vanadium atoms, V(1) and V(2), occupy general positions, with the V(1) atoms only slightly displaced from centers of inversion. The two vanadium atoms are located in slightly deformed octahedra (see Figures 2 and 3 and Table IV); in addition, both are displaced off the equatorial plane of their octahedra and form one short and one long vanadium–oxygen bond, as is char-

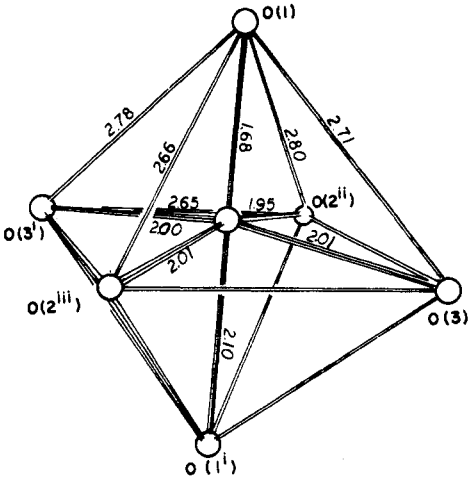

Figure 2. V(1) octahedron.

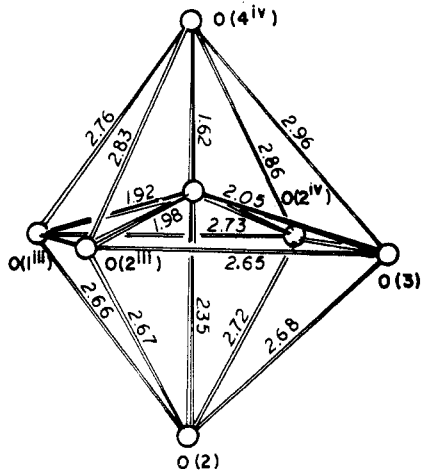

Figure 3. V(2) octahedron.

acteristic of many vanadium–oxygen compounds.[28-30] The difference is more pronounced for the V(2) octahedra (V–O = 2.35 and 1.62 Å) than for the V(1) octahedra (V–O = 2.10 and 1.68 Å), since the oxygen atom in the short V(2)–O bond is not shared by any other vanadium atoms. The octahedra are linked together by edge, corner, and face sharing to form 6 Å thick sheets that extend parallel to (100). In each sheet, the vanadium atoms lie on three parallel planes; the central plane is composed of V(1) atoms (two per unit cell) and is adjoined on either side by a plane of V(2) atoms (four per unit cell). In every plane of vanadium atoms, the octahedra are linked by corner sharing with two neighboring octahedra into infinite zigzag chains. Each V(1) octahedron also shares four of its edges and four of its corners with eight V(2)-occupied octahedra. Each V(2) shares two edges and two corners with four V(1)-occupied neighboring octahedra and one face and one edge with two other V(2)-occupied octahedra lying across the V(1) plane (see Figure 4). The most distinct feature of the structure are the pairs of V(2) atoms in face-shared octahedra. These vanadium atoms are 2.92 Å apart across the shared face and are connected to adjacent pairs by corner sharing (along c_0 with V(2)–V(2) = 3.49 Å, V(2)–O–V(2) = 123.3°) and by edge sharing (across the V(1) plane, with V(2)–V(2) = 3.43 Å) and are separated along b_0 by strings of V(1) octahedra (V(2)–V(1) = 3.01 Å, edge sharing; V(2)–V(1) = 3.72 Å, corner sharing).

Between these sheets, zigzag chains of ammonium ions infinitely extend (with N···N = 3.66 (1) Å) parallel to (100). This complex pattern of polyhedra sharing with the formation of tunnels large enough for cation occupancy is a variation of

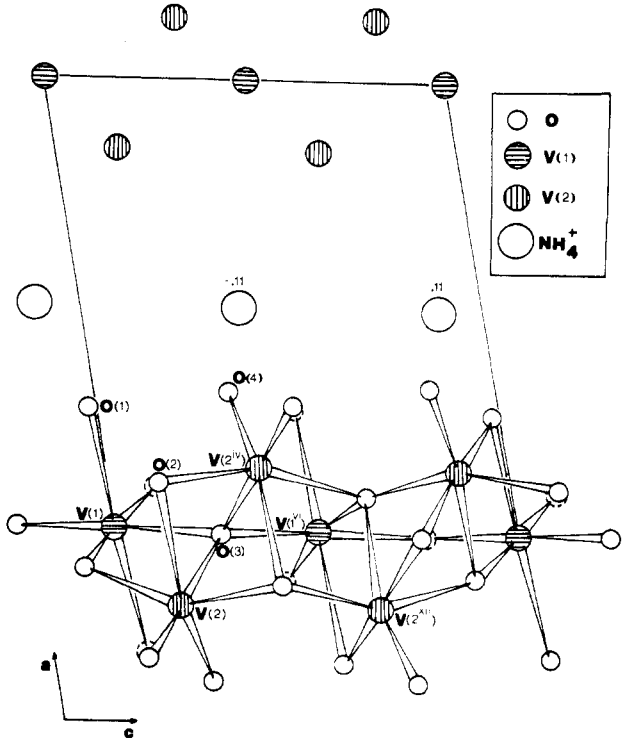

Figure 4. Projection of the structure of $NH_4V_3O_6F$ on the (010) plane. The V(1) atoms are at a height of $y = 0$ and 1 and V(2) are at $y = 0.5$ and -0.5.

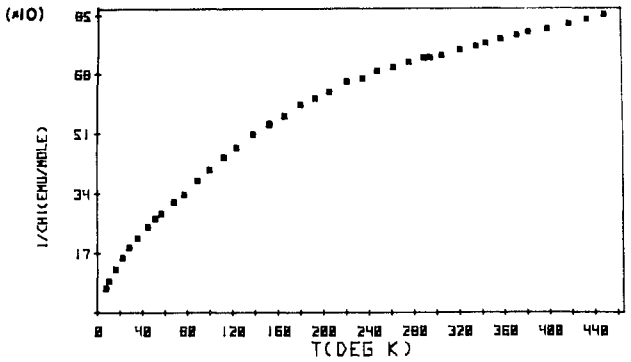

Figure 5. Inverse susceptibility vs. temperature for $NH_4V_3O_6F$.

the pattern seen in many of the vanadium oxides and bronzes.[31-33]

Alternatively, the structure may be viewed as consisting of distorted hexagonally close-packed layers of oxygen atoms and ammonium ions parallel to (101) with three-eights of the octahedral holes filled by vanadium atoms. As expected, all of the octahedral holes with only oxygen nearest neighbors are occupied, whereas any holes that would include ammonium ions as neighbors are vacant. The c/a ratio $(2(a_0 + c_0)/(a_0 - c_0))$ of 1.67 for these planes is close to the ideal value of 1.63 indicating that the distortion of the oxygen and ammonium lattice from a hexagonally close-packed arrangement is small.

The fluorine atoms were assumed to be randomly disordered over the four oxygen sites. The individual anion environments are included in Table IV.

Physical Properties

Discussion. The plot of χ^{-1} vs. T is presented in Figure 5. The material shows Curie–Weiss behavior in the temperature range 240–450 K with a P_{eff} of 1.83 BM, as compared to a theoretical spin-only moment of 1.73 BM for a d^1 system.

Honda–Owens measurements at 4.2 and 77 K show that the susceptibility is field independent, which indicates the

Table IV. Interatomic Distances (Å) and Angles (deg)[a]

(a) Oxygen Approaches in V(1) Octahedra

O(1)···O(3)	2.71 (1)	O(1)···O(2^{ii})	2.80 (1)
O(1)···O(3^{i})	2.78 (1)	O(2^{ii})···O(3)	2.96 (1)
O(1)···O(2^{iii})	2.66 (1)	O(2^{ii})···O(3^{i})	2.65 (1)

(b) V(1)–O Distances

V(1)–O(1^{i})	2.10 (1)	V(1)–O(3)	2.01 (1)
V(1)–O(2^{ii})	1.95 (1)	V(1)–O(3^{i})	2.00 (1)
V(1)–O(2^{iii})	2.02 (1)	V(1)–O(1)	1.68 (1)

(c) Oxygen Approaches in V(2) Octahedra

O(4^{iv})···O(3)	2.96 (1)	O(1^{iii})···O(2^{iii})	2.83 (1)
O(4^{iv})···O(2^{iv})	2.86 (1)	O(2^{iii})···O(3)	2.65 (1)
O(4^{iv})···O(1^{iii})	2.76 (1)	O(2)···O(3)	2.68 (1)
O(4^{iv})···O(2^{iii})	2.83 (1)	O(2)···O(2^{iv})	2.72 (1)
O(2^{iv})···O(3)	2.68 (1)	O(2)···O(1^{iii})	2.66 (1)
O(2^{iv})···O(1^{iii})	2.73 (1)	O(2)···O(2^{iii})	2.67 (1)

(d) V(2)–O Distances

V(2)–O(1^{iii})	1.92 (1)	V(2)–O(2^{iv})	1.99 (1)
V(2)–O(2)	2.35 (1)	V(2)–O(3)	2.05 (1)
V(2)–O(2^{iii})	1.98 (1)	V(2)–O(4^{iv})	1.62 (1)

(e) O–V(2)–O Angles

O(2)–V(2)–O(2^{iv})	178.0 (3)	O(2^{iii})–V(2)–O(2^{iv})	151.4 (4)
O(3)–V(2)–O(1^{iii})	151.0 (3)		

(f) O–V(1)–O Angles

O(1)–V(1)–O(1^{i})	177.2 (4)	O(3)–V(1)–O(3^{i})	167.8 (2)
O(2^{ii})–V(1)–O(2^{iii})	167.8 (2)		

(g) Nitrogen Separation along Chains

N^{ii}···N^{v}	3.66 (1)

(h) V(1) Environment

Corner Sharing with V(1) Neighbors (Same Plane)

V(1)···V(1^{vi})	3.494 (5)	V(1)–O(3)–V(1^{vi})	121.0 (4)

Corner Sharing with V(2)

V(1)···V(2^{iv})	3.560 (5)	V(1)–O(3)–V(2^{iv})	122.2 (2)
V(1)···V(2^{vii})	3.710 (5)	V(1)–O(2^{ii})–V(2^{vii})	140.6 (4)
V(1)···V(2^{viii})	3.726 (5)	V(1)–O(3^{i})–V(2^{viii})	133.7 (2)
V(1)···V(2^{ix})	3.748 (5)	V(1)–O(2^{iii})–V(2^{ix})	138.4 (3)

Edge Sharing with V(2)

V(1)···V(2^{i})	2.995 (6)	V(1)···V(2)	3.025 (5)
V(1)···V(2^{iii})	2.923 (6)	V(1)···V(2^{ii})	3.197 (5)

(i) V(2) Environment

Corner Sharing with V(2) Neighbors (Same Plane)

V(2)···V(2^{xii})	3.495 (4)	V(2)–O(2^{iv})–V(2^{xii})	123.3 (3)

Corner Sharing with V(1)

V(2)···V(1^{vi}) or	3.726 (5)	V(2)–O(3)–V(1^{vi}) or	133.7 (2)
V(2)···V(1^{iv})	3.560 (5)	V(2)–O(3)–V(1^{iv})	122.2 (2)
V(2)···V(1^{xi}) or	3.710 (5)	V(2)–O(2^{iv})–V(1^{xi}) or	140.6 (4)
V(2)···V(1^{xii})	3.748 (5)	V(2)–O(2^{iv})–V(1^{xii})	138.4 (3)

Edge Sharing with V(1)

V(2)···V(1) or	3.025 (5)	V(2)···V(1^{xi}) or	3.205 (5)
V(2)···V(1^{i})	2.895 (6)	V(2)···V(1^{iii})	3.197 (5)
	2.995 (6)		2.923 (6)

Edge Sharing with V(2)

V(2)···V(2^{iii})	3.427 (3)

Face Sharing with V(2)

V(2)···V(2^{iv})	2.924 (4)

(j) Anion Environment

Distances

O(1)–V(1) or	1.68 (1)	O(3)–V(1) or	2.01 (1)
O(1)–V(1^{i})	2.10 (1)	O(3)–V(1^{i})	2.00 (1)
O(1)–V(2^{iii})	1.92 (1)	O(3)–V(1^{vi}) or	2.00 (1)
O(1)···O(2^{iii})	2.66 (1)	O(3)–V(1^{iv})	2.01 (1)
O(1)···O(3)	2.71 (1)	O(3)–V(2)	2.05 (1)
O(1)···O(2^{ix})	2.73 (1)	O(3)–V(2^{iv})	2.05 (1)
O(1)···O(4^{ix})	2.76 (1)	O(3)···O(2^{iii})	2.65 (1)
O(1)···O(3^{i})	2.78 (1)	O(3)···O(2^{xii})	2.65 (1)
O(1)···O(2^{ii})	2.80 (1)	O(3)···O(2)	2.68 (1)
O(1)···O(2)	2.83 (1)	O(3)···O(2^{iv})	2.68 (1)
O(1)···O(4)	2.96 (1)	O(3)···O(1)	2.71 (1)
O(1)···O(4^{viii})	3.01 (1)	O(3)···O(1^{iv})	2.71 (1)
O(1)···N^{ii}	3.06 (1)	O(3)···O(1^{i})	2.78 (1)
O(1)···N^{v}	3.20 (1)	O(3)···O(1^{vi})	2.78 (1)
O(1)···O(4^{xiii})	3.79 (1)	O(3)···O(2^{ii})	2.96 (1)
O(2)–V(1^{x}) or	1.95 (1)	O(3)···O(2^{vii})	2.96 (1)
O(2)–V(1^{iii})	2.02 (1)	O(3)···O(4)	2.96 (1)
O(2)–V(2^{iii})	1.98 (1)	O(3)···O(4^{iv})	2.96 (1)
O(2)–V(2^{iv})	1.99 (1)	O(4)–V(2)	1.62 (1)
O(2)–V(2)	2.35 (1)	O(4)···O(1^{xii})	2.76 (1)
O(2)···O(3^{v})	2.65 (1)	O(4)···O(2^{xii})	2.83 (1)
O(2)···O(1^{iii})	2.66 (1)	O(4)···O(2)	2.86 (1)
O(2)···O(2^{iii})	2.67 (1)	O(4)···N^{ii}	2.91 (1)
O(2)···O(3)	2.68 (1)	O(4)···N^{xii}	2.95 (1)
O(2)···O(2^{iv})	2.72 (1)	O(4)···O(1)	2.96 (1)
O(2)···O(1^{xii})	2.73 (1)	O(4)···O(3)	2.96 (1)
O(2)···O(1^{x})	2.80 (1)	O(4)···O(1^{vi})	3.01 (1)
O(2)···O(4^{ix})	2.83 (1)	O(4)···O(4^{xiv})	3.06 (1)
O(2)···O(1)	2.83 (1)	O(4)···N	3.08 (1)
O(2)···O(4)	2.86 (1)	O(4)···O(4^{xiii})	3.40 (1)
O(2)···O(3^{x})	2.96 (1)	O(4)···O(1^{xiii})	3.79 (1)
O(2)···N	3.43 (1)		

Angles

V(1)–O(1)–V(2^{iii}) or	108.3 (3)	V(1)–O(3)–V(1^{vi})	121.0 (3)
V(1^{i})–O(1)–V(2^{iii})	105.6 (2)	V(1)–O(3)–V(2)	96.1 (3)
V(1^{x})–O(2)–V(2^{iii}) or	94.9 (3)	V(1)–O(3)–V(2^{iv})	122.2 (2)
V(1^{iii})–O(2)–V(2^{iii})	98.3 (3)	V(1^{vi})–O(3)–V(2)	133.7 (2)
V(1^{x})–O(2)–V(2^{iv}) or	140.6 (4)	V(1^{vi})–O(3)–V(2^{iv})	91.2 (3)
V(1^{iii})–O(2)–V(2^{iv})	138.4 (3)	V(2)–O(3)–V(2^{iv})	90.9 (2)
V(2^{iii})–O(2)–V(2^{iv})	123.3 (3)		

[a] The atoms are numbered as in Table II.

absence of any ferromagnetic impurities. The Weiss constant Θ has a value of −622 K, but no Néel point was observed down to 4.2 K. These facts indicated that strong but short-range antiferromagnetic exchange interactions exist down to 4.2 K.

The electrical resistivity of single crystals of $NH_4V_3O_6F$ is anisotropic. The resistivity is too high to be measured perpendicular to (100) (across the strings of ammonium ions), whereas parallel to the (100) plane the resistivity has a minimum room-temperature value of 10^8 Ω-cm. As a result of the high room-temperature resistivity and the low decomposition temperature of $NH_4V_3O_6F$ (498 K), it was not possible to obtain a meaningful determination of the resistivity as a function of temperature. Both the Curie–Weiss behavior of the susceptibility and the high resistivity of the material appear to be consistent with localized electron character.

Goodenough[9] has shown that for transition metal oxides (where $n_{t_{2g}} \leq 3$) in which the transition metal cation is in an octahedral (or distorted octahedral) interstice, two types of cooperative phenomena which will result in antiferromagnetic behavior are possible: a direct cation–cation interation (via

overlap of the cation t_{2g} or hybridized t_{2g} orbitals) and cation–anion–cation π-bond interactions (via covalent mixing of the cation e_g and anion p orbitals).

In $NH_4V_3O_6F$, both cation–cation and cation–anion–cation interactions are present. In the 6 Å thick sheets of vanadium octahedra (Figure 4), the closest V–V approaches ($V(2)–V(2^{iv})$ = 2.92 Å) occur between pairs of face-shared octahedra, in planes perpendicular to [010]. The pairs of face-shared octahedra are connected to each other along the c_0 direction by corner sharing ($V(2)–V(2^{xii})$ = 3.49 Å, $V(2)–O(2^{ix})–V(2^{xii})$ = 123.3°) and across the V(1) planes by edge sharing ($V(2)–V(2^{iii})$ = 3.43 Å). Along b_0, the pairs of face-shared octahedra are linked via edge and corner sharing with intermediate V(1) octahedra. The average edge-sharing V(2)–V(1) separation is 3.01 Å. The zigzag chains of ammonium ions that run parallel to (100) separate the 6 Å thick sheets of vanadium octahedra (Figure 4) and preclude any extended interactions perpendicular to the plane. Thus, even though the vanadium atoms in the face-shared octahedra are close enough to propagate extended interactions, the path of the interactions is limited by the environment around the face-shared pairs. Whereas there may be localized antiferromagnetic coupling of the vanadium atoms in the face-shared pairs, the magnetic data indicate that extended vanadium–oxygen–vanadium interactions do not occur down to 4.2°K. Therefore, the antiferromagnetic character of the material is apparently due to the direct vanadium–vanadium interactions between the face-shared pairs, and the vanadium–oxygen–vanadium interactions do not play a significant role. In addition, the high resistivity of $NH_4V_3O_6F$ is a reflection of the localized electron character. This is an unusual behavior for a V^{4+} (d^1) system.

Acknowledgment. This work was supported by the National Science Foundation (Grant No. GP 26617) and the Materials Research Laboratory Program at Brown University. The authors wish to thank Professors G. B. Carpenter, R. J. Arnott, and Dr. J. Steger for their helpful discussions.

Registry No. $NH_4V_3O_6F$, 57484-03-4; ammonium vanadate, 7803-55-6; vanadium, 7440-62-2; ammonium hydrogen fluoride, 1341-49-7.

Supplementary Material Available: Listing of structure factor amplitudes (3 pages). Ordering information is given on any current masthead page.

References and Notes

(1) H. Sorum, *Forh., K. Nor. Vidensk. Selsk.*, **16**, 39 (1943).
(2) H. T. Evans, Jr., *Z. Kristallog., Kristallgeom., Kristallphys., Kristallchem.*, **114**, 257 (1960).
(3) H. T. Evans, Jr., *Acta Crystallogr.*, **13**, 1019 (1960).
(4) H. G. Bachmann and W. M. Barnes, *Z. Kristallogr., Kirstallgeom., Kristallphys., Kristallchem.*, **115**, 215 (1961).
(5) A. D. Wadsley, *Acta Crystallogr.*, **10**, 261 (1957).
(6) G. Andersson, *Acta Chem. Scand.*, **10**, 623 (1956).
(7) A. Carpy and J. Galy, *Bull. Soc. Fr. Mineral. Cristallogr.*, **94**, 24 (1971).
(8) "International Tables for X-Ray Crystallography", Vol., III, Kynoch Press, Birmingham, England, 1962, p 277.
(9) J. B. Goodenough, *Phys. Rev.*, **117**, 1442 (1960).
(10) R. D. Shannon and C. T. Prewitt, *Acta Crystallogr., Sect. B*, **25**, 925 (1969).
(11) M. L. F. Bayard, T. G. Reynolds, M. Vlasse, H. L. McKinzie, R. J. Arnott and A. Wold, *J. Solid State Chem.*, **3**, 484 (1971).
(12) B. L. Chamberland, *Mater. Res. Bull.*, **6**, 425 (1971).
(13) J. Galy and A. Carpy, *C. R. Hebd. Seances Acad. Sci., Ser. C*, **268**, 2195 (1969).
(14) B. L. Chamberland, A. W. Sleight, and W. H. Cloud, *J. Solid State Chem.*, **2**, 49 (1971).
(15) F. Pintchovski, S. Soled, R. Lawler, and A. Wold, *Inorg. Chem.*, **14**, 1390 (1975).
(16) G. H. Walden, Jr., L. P. Hammett, and S. M. Edmonds, *J. Am. Chem. Soc.*, **56**, 57 (1934).
(17) D. G. Wickam and E. R. Whipple, *Talanta*, **10**, 314 (1963).
(18) R. L. Adams, Ph.D. Thesis, Brown University, 1973.
(19) B. Morris and A. Wold, *Rev. Sci. Instrum.*, **39**, 1937 (1968).
(20) A. Catalano, Ph.D. Thesis, Brown University, 1973.
(21) P. W. Selwood, "Magnetochemistry", Interscience, New York, N.Y., 1956, p 78.
(22) L. J. van der Pauw, *Philips Res. Rep.*, **13**, 1 (1968).
(23) W. C. Hamilton, *Acta Crystallogr.*, **10**, 629 (1956).
(24) W. R. Busing, K. O. Martin, and H. A. Levy, Report ORNL-TM-305, Oak Ridge National Laboratory, Oak Ridge, Tenn.
(25) D. T. Cromer and J. T. Waber, *Acta Crystallogr.*, **18**, 104 (1965).
(26) D. T. Cromer, *Acta Crystallogr.*, **18**, 17 (1965).
(27) Supplementary material.
(28) G. Andersson, *Acta Chem. Scand.*, **10**, 623 (1956).
(29) M. Horiiuchi, M. Tokonami, N. Morimoto, and K. Nagasawa, *Acta Crystallogr., Sect. B*, **28**, 1404 (1972).
(30) J. M. Longo and R. J. Arnott, *J. Solid State Chem.*, **1**, 269 (1973).
(31) J. C. Bouloux and J. Galy, *Acta Crystallogr., Sect. B*, **29**, 269 (1973).
(32) J. Galy and D. Lavaud, *Acta Crystallogr., Sect. B*, **27**, 1005 (1971).
(33) P. Hagenmuller, J. Galy, M. Pouchard, and A. Casalot, *Mater. Res. Bull.*, **1**, 45 (1966).